Chemical Science

Accepted Manuscript

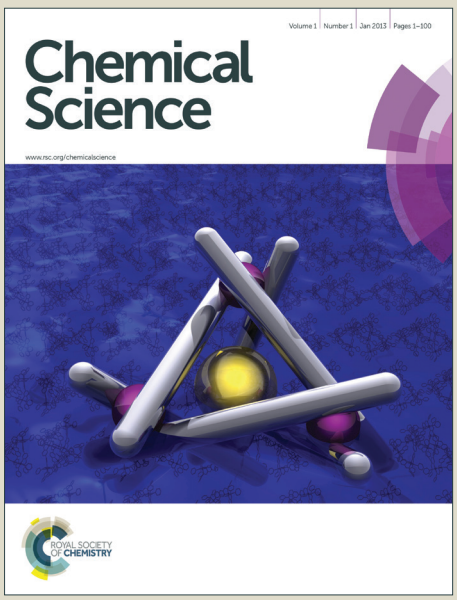

ROYAL SOCIETY OF CHEMISTRY

www.rsc.org/chemicalscience

Chemical Science

ARTICLE

Mechanical energy storage performances of the Aluminum Fumarate Metal–Organic Framework

Received 00th January 20xx,
Accepted 00th January 20xx

DOI: 10.1039/x0xx00000x

www.rsc.org/

Pascal. G. Yot,[*a] Louis Vanduyfhuys,[b] Elsa Alvarez,[c, d] Julien Rodriguez,[e] Jean-Paul Itié,[f] Paul Fabry,[c] Nathalie Guillou,[c] Thomas Devic,[c] Isabelle Beurroies,[f] Philip L. Llewellyn,[f] Veronique Van Speybroeck,[b] Christian Serre,[c] Guillaume Maurin,[a]

The aluminum Fumarate MOF A520 or MIL-53-FA is revealed as a promising material for mechanical energy-related applications with performances in terms of work and heat energies which surpass that of any porous solids reported so far. Complementary experimental and computational tools are deployed to finely characterize and understand the pressure-induced structural transition at the origin of this unprecedented level of performances.

1. Introduction

Metal organic frameworks (MOFs) have aroused a great interest over the past decade not only for the wide spectrum of materials that can be synthesized but also for their potential use in societally-relevant applications.[1] While much effort has been focused to the design of MOFs for gas storage/separation applications, [1] much less attention has been paid to tune their mechanical energy storage performances.[2-10] Indeed, very few hydrophobic MOFs have been reported to absorb relatively high amounts of energy during water intrusion-exclusion cycles.[9,10] Alternatively, flexible MOFs have been proposed as potential nano-dampers or shock absorbers since their pressure-induced structural transitions towards a contracted phase can generate relatively high work energy during compression/decompression cycles.[2-8] In particular, Hg-porosimetry and high-pressure X-ray diffraction experiments revealed that the carboxylate-based MIL-53 series [2,4,7,8] rival or even surpass the mesoporous silica and zeolites [9-13] in terms of mechanical energy stored. Very recently, some of us have significantly improved the crystallinity of the commercialized Aluminum fumarate A520 [14-18] via an optimized synthesis route which rendered possible the resolution of the crystal structure of this solid in its hydrated form. This solid denoted as MIL-53(Al)-FA was revealed to be isoreticular of the well documented highly flexible MIL-53(Al)-BDC (BDC=1,4-benzenedicarboxylate) with a slightly smaller pore dimension (7.3 x 7.7 $Å^2$ vs 8.5 x 8.5 $Å^2$) [19], and interestingly a rigid character upon water sorption. Following the strong shift to higher pressure observed previously when turning from the highly flexible MIL-53(Cr, Al) solids to the 'sorption rigid' parent MIL-47(V^{IV}) analogue,[4] we assumed here that one could use the Al fumarate features as an attractive candidate to maximize the work energy (W = P × ΔV) absorbed during one compression-decompression cycle by an expected increase in the structural transition pressure (P) while maintaining a relatively high volume variation (ΔV).[1]

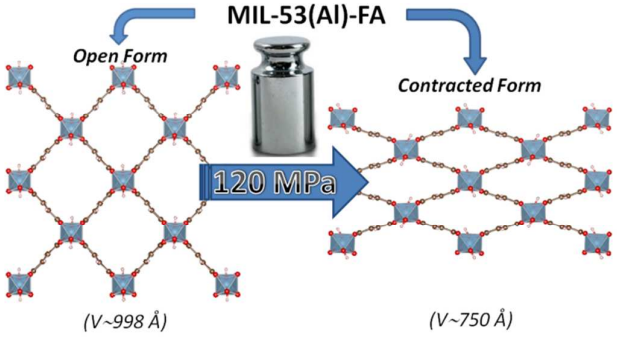

Fig. 1 *Schematic representation of the pressure-induced contraction of MIL-53(Al)-FA between an open and a contracted form.*

Hg-porosimetry and in situ high-pressure Synchrotron X-ray powder diffraction coupled with molecular simulations

[a] Institut Charles Gerhardt Montpellier UMR 5253 CNRS UM ENSCM, Université de Montpellier, CC 15005, Place Eugène Bataillon, F-34095 Montpellier cedex 05, France. e-mail: pascal.yot@umontpellier.fr; Tel.: +33 4 67 14 32 94; Fax: +33 4 67 14 42 90.
[b] Centre for Molecular Modeling, Ghent University, Technologiepark 903, B-9052 Zwijnaarde, Belgium. Centre for Molecular Modeling, Ghent University, Technologie park 903, B-9052 Zwijnaarde, Belgium.
[c] Institut Lavoisier Versailles, Université de Versailles St-Quentin, 45, avenue des Etats-Unis, F-78035 Versailles cedex, France.
[d] PSA Peugeot Citroën - Direction Scientifique et Technologies Futures. DSTF/SEPC/STEP. Route de Gisy - 78943 Velizy-Villacoublay cedex, France.
[e] Aix-Marseille Université, CNRS, MADIREL (UMR 7246), Centre Scientifique de St. Jérôme, F-13397 Marseille cedex 20, France.
[f] Synchrotron Soleil, L'orme des Merisiers, Saint-Aubin - BP 48, F-91192 Gif-sur-Yvette cedex, France.
Electronic Supplementary Information (ESI) available: Experimental procedures, X-ray diffraction, and molecular simulation. See DOI: 10.1039/x0xx00000x

confirmed that the dehydrated version of MIL-53(Al)-FA shows a reversible structural contraction under an applied pressure above 100 MPa. This leads to a very high work energy of 60 J/g that considerably exceeds the values reported so far for other porous solids.[2-13] This unprecedented level of performance is maintained with the use of silicon oil, a more environmental friendly fluid, to perform the compression-decompression cycles. A direct measurement of the heat energy confirms the great promise of this low-cost and stable MOF for such an application.

2. Material and methods

Powder of Aluminum Fumarate Metal–Organic Framework MIL-53-FA has been prepared following the optimized synthesis route very recently reported by Alvarez *et al*.[18] The pressure-induced structure response of both hydrated and hydrated solids was characterized by mercury intrusion experiments [2,4,7] using a mercury porosimeter Micromeritics Autopore 9240. Two intrusion-extrusion (compression-decompression) cycles were applied on the samples in the pressure range 10^{-4}-420 MPa (see ESI). Angle-dispersive X-ray powder diffraction (XRPD) data at high pressure (up to 1.88 GPa) was performed in-house using filtered Mo-K_α (λ=0.710730 Å) and at PSICHE beamline of the Synchrotron Soleil (Saint-Aubin, France) using a monochromatic beam (50×50 μm^2) with a wavelength of λ=0.37380 Å. The pressure was generated with a membrane diamond anvil cell (MDAC) using silicon oil AP 100 (Aldrich) as pressure-transmitting medium as its kinetic diameter largely exceeds the window size of the fumarate which ensures that it does not enter inside the pores. The applied pressure was determined from the shift of the ruby R1 fluorescence line.[20] The heat related to the pressure-induced structural transition of the dehydrated solid was determined using a specifically devised calorimetry system [8] using silicon oil as pressure-transmitting medium.

Molecular simulations were performed to provide a structure model of the contracted phase detected under applied pressure. This computational effort was based on a newly *ab initio* derived flexible force-field for the MOF framework using the QuickFF protocol.[21] All the details about experiments and modelling are available in ESI.

3. Results and discussion

The mechanical behavior of the hydrated MIL-53(Al)-FA was first explored by mercury intrusion and angle dispersive XRPD. Figure S1 reports the evolution of the cumulative volume of intruded mercury as a function of the applied pressure after two intrusion–extrusion (compression–decompression) cycles. Apart from the increase of the volume of Hg intruded below 10 MPa assigned to the compaction of the powder and the filling of the interparticular porosity, this curve does not show any step at higher pressure up to 420 MPa. This observation emphasizes that the hydrated solid does not undergo any structural change in this range of pressure. This holds also true at higher pressure as evidenced by the XRPD patterns collected on this solid which remains unchanged up to 1.88 GPa (Figure S2). Referring to our previous computational investigation on the guest-modulation of the mechanical properties of MIL-53(Cr),[22] the absence of a structural phase transition is not necessarily due to the intrinsic robustness of the MOF framework but rather to the internal stress exerted by the water molecules which tends to put up resistance to the external applied pressure. To confirm this, the solid was further investigated in its dehydrated form. A structure model was first constructed starting with the crystal structure of the hydrated form and subsequently optimized by Density Functional Theory (DFT) calculations in the absence of the free water molecules (see ESI). This led to a structure with the same monoclinic symmetry (SG $P2_1/c$) and a unit cell volume of 985 $Å^3$ in good agreement with the experimental value (998.0(1) $Å^3$) obtained from a XRPD pattern indexing (see Figure S3). Mercury porosimetry experiments performed on this solid (Figure 2) revealed a progressive increase of Hg intruded between 110 MPa and 400 MPa assigned to a contraction of the structure since Hg cannot penetrate the micropores.

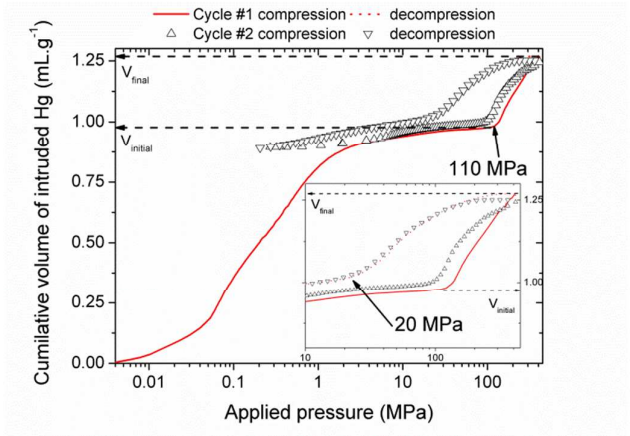

Fig. 2 *Cumulative volume of intruded mercury in two intrusion-extrusion cycles as a function of the applied pressure obtained for the dehydrated MIL-53(Al)-FA solid ($V_{initial}$ and V_{final} are the volumes of mercury intruded before and after the contraction of the solid respectively).*

High pressure XRPD experiments further confirmed a structural change in the same range of pressure with the appearance of new Bragg peaks above 250 MPa (Figure 3) that are assigned to a more contracted form of MIL-53(Al)-FA. For the pressures above 410 MPa the XRPD patterns most probably correspond to the contracted pore form although the presence of a small fraction of the initial structure is likely to occur. The experimental resolution was not of sufficient quality to allow an indexation of the unit cell parameters for the contracted pore structure. It was however possible to estimate the unit cell volume of the contracted phase using the Hg-porosimetry data since we have previously evidenced that the unit cell volume change of the MIL-53 analogues [2,4,7,8] correlates well the increase of the volume of intruded Hg. The

increase in volume of mercury during the compression step is 0.25 mL.g^{-1}. Considering a unit cell volume of 998 Å^3 for the pristine dehydrated structure, this leads to a contracted structure with a unit cell volume of ~750 Å^3 which is significantly smaller than the cell dimensions of the pressure-induced phases previously observed for MIL-53(Al)-BDC (820 Å^3),[7] MIL-53(Cr)-BDC (931 Å^3) [23] and its MIL-47(V) (950 Å^3) [4] analogue. Such as contraction is due both to the decrease of cell parameter associated with the presence of a shorter fumarate spacer *vs* benzyl groups for MIL-53's, as well as the resulting absence of strong π-π interactions that contribute in MIL-53's to resist towards a more pronounced closure of the system.

A computational effort has been further deployed to propose a structural model for this contracted phase. Based on a newly *ab initio* flexible force-field derived for the MOF framework (see ESI), the energy profile of the MIL-53(Al)-FA structure as a function of its unit cell volume was calculated at 0 K (Figure S6). The optimized geometry at a fixed volume of 750 Å^3 encountered during this energy scan was proposed as a plausible structure model for this contracted phase. The consistency obtained between the theoretical XRPD pattern calculated for this predicted structure and the corresponding experimental data collected at 410 MPa (Figure S4) confirmed that the appearance of the new Bragg peaks is due to a contraction of MIL-53(Al)-FA and that the proposed structure model is reliable. In a similar way to the MIL-53-BDC analogues, the structural contraction leads to a significant decrease of the Al-Oc-Cc-Cg2 dihedral angle from 180° (pristine phase) to 155° (contracted phase). This emphasizes that the rotation of the linker about the Oc-Oc axis is also the driving force for the structural transition of MIL-53(Al)-FA.[4, 7, 24]

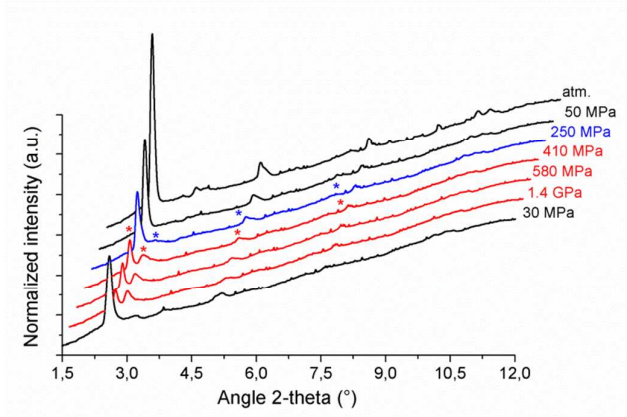

Fig. 3 *X-ray powder diffraction patterns of the MIL-53(Al)-FA as a function of the applied pressure (λ=0.37380 Å). Patterns in black correspond to the pure open form, in blue mixture of open and contracted pore forms (* indicate the diffraction peaks assigned to the contracted form) and in red contracted form although the presence of a small concentration of open form is likely to occur).*

The compression step occurs at a pressure which is significantly higher than that observed either for MIL-53(Al)-BDC (55 MPa), MIL-53(Cr)-BDC (55 MPa), or MIL-47(V)-BDC (85 MPa). This implies that the work energy stored by MIL-53(Al)-FA that can be calculated from the pressure transition and the corresponding volume variation, attains 60 J.g^{-1}. This value largely exceeds the performances of the Al-BDC analogue by one order of magnitude and makes MIL-53(Al)-FA as the best porous solid reported so far for such an application (see Table 1).

Table 1 *Comparison of the work energy performance of MIL-53(Al)-FA, with that of other porous solids.*

	Work (J.g^{-1})	$P_{transition}$ (MPa)	Reference
MIL-53(Al)-FA	60	110	This work
MIL-53(Al)-BDC	7	18	7
MIL-53(Cr)-BDC	16	55	2
MIL-47(V)-BDC	33	125	4
ZIF-8	13.3	-	10
Silicalite	11	-	25
SBA-15 mesoporous silica	4.3-6.1	-	26

Noteworthy, unlike for MIL-53(Al) whereas the transition was found to be irreversible, Mercury intrusion further evidenced that MIL-53(Al)-FA shows a fully reversible mechanical behavior upon compression-decompression cycles with the presence of a hysteresis of about 125 MPa. This was confirmed by high pressure XRPD which revealed that the contracted version of MIL-53(Al)-FA returns to the initial form once the pressure is released (Figure 3). Correlated with its industrial availability (A520), these observations make this solid an exceptional candidate for mechanical energy storage applications and particularly in the form of nano-dampers. However for application purposes, mercury cannot be considered as pressure transmitting medium due to very high toxicity. We envisaged as a further step the use of a more friendly environmental fluid, the silicon oil to perform cycles of compression/decompression on MIL-53(Al)-FA (see ESI). The corresponding data are reported in Figure 4.

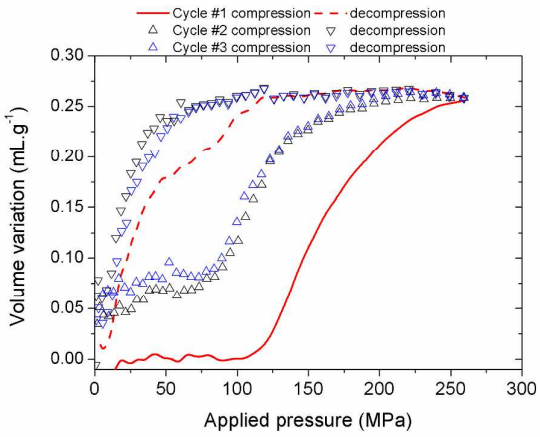

Fig. 4 *Volume variation of MIL-53(Al)-FA as a function of the applied oil pressure during three compression-decompression cycles.*

In contrast with the Hg experiment, the increase of the volume at low pressure is not present anymore as the silicone oil is a wetting fluid that can spontaneously occupy the interparticular

porosity. A step for cycle 1 occurs in the pressure range [100-250 MPa] and leads to a volume variation of 0.25 mL/g^{-1}. Both observations concur very well with the values obtained with mercury porosimetry, the lower upper pressure vs Hg being associated with the limit of the current oil system (250 MPa) compared to the mercury set-up (400 MPa). This strongly supports that the selected silicon oil is bulky enough not to penetrate into the MOF micropores and hence this fluid can be used to allow the monitoring of the pressure-induced structural transition of MIL-53(Al)-FA.

The silicon oil compression-decompression cycle presents a hysteresis consistent with the Hg porosimetry and the work energy stored 41.7 J.g^{-1} remains very high. Both features confirm the promise of this solid as a potential nano-damper. A partial loss of volume and a decreasing of the transition pressure are recorded after the first compression (from 0.25 mL.g^{-1} and 100-250 MPa for the first cycle to 0.20 mL.g^{-1} and 72-250 MPa for other cycles respectively) which might be due to the presence of silicon oil at the pore aperture of the MOF at the outer surface of the particles.[8] However, the performances in terms of work energy stored remain very high (22.9 J.g^{-1}, see Table 2) and the cycles are superimposable, within experimental error.

The heat dissipated by the structural transition of the MIL-53(Al)-FA during the first compression/decompression cycle was further assessed by calorimetry measurements. The corresponding data are reported in Figure 5.

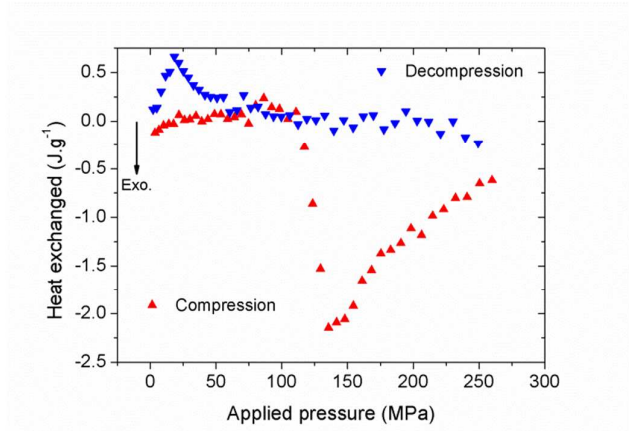

Fig. 5 *Heat energy obtained for MIL-53(Al)-FA as a function of the pressure during the first cycle release. Red up-triangles correspond to compression and blue down-triangles decompression.*

It is shown that the compression (contraction of the structure) is exothermic while the decompression (expansion of the structure) is endothermic and this trend is consistent with that previously reported for MIL-53(Al)-BDC.[8] Table S1 evidences that in terms of dissipated heat energy, MIL-53(Al)-FA also largely outperforms all the porous solids, i.e. other MOFs and hydrophobic silica. It is also shown that after the first cycle, the heating energy (i.e. difference in heat of compression and decompression energy) is around -18.7 J.g^{-1} which is significantly higher that the value obtained for MIL-53(Al)-BDC (-5 to -6 J.g^{-1} during cycle 1).[8]

This suggests that a heat evacuation protocol would need to be implemented for the use of this solid as nano-damper. Finally, Table 1 emphasizes that the work and heat energies are significantly different resulting in internal energy (U) (-8.4 to 6.9 J g^{-1}) much higher than the value previously reported for MIL-53(Al)-BDC (-3.0 to 1.0 J g^{-1}).

Table 2 *Experimental energetic data of compression/decompression cycles on the MIL-53(Al)-FA.*

	Work (J.g^{-1})	Heat (J.g^{-1})	Internal energy (J.g^{-1})
Cycle 1: Compression	41.7	-25.1	16.6
Cycle 1: Decompression	-10.8	6.4	-4.4
Cycle 2: Compression	22.9	-18.7	4.2
Cycle 2: Decompression	-8.0	6.3	-1.7
Cycle 3: Compression	22.2	-18.2	4.0
Cycle 3: Decompression	-8.8	6.5	-2.3

Conclusions

The Aluminum Fumarate MIL-53-FA or A520 represents the best porous solid reported so far for mechanical-energy related applications, by virtue of its reversible structural switching towards a more contracted phase that can be provoked by the application of a high external pressure, with outstanding performances in terms of work and heat energies. This commercialized material is particularly attractive since its low-production cost, low toxicity and high stability will be not a drawback for further device development following the concept of MOF/silicon oil system proposed in this study.

Acknowledgements

The authors would like to thank the French National Agency for Research ANR "MODS" (ANR-12-BS10-0005) for its financial supports. Dr. J. Haines (ICGM) is also thanked for his support for X-ray diffraction on hydrated form of MIL-53(Al)-FA. We acknowledge the French national synchrotron radiation source "Synchrotron Soleil" (Saint-Aubin, France) and PSICHE beamline for beam time. Renaud Denoyel (MADIREL) is thanked for his aid with calculations of energy data. G.M. thanks Institut Universitaire de France for its support. VVS and LV acknowledge support from the Fund for Scientific Research - Flanders (FWO), the Research Board of Ghent University (BOF). V. Van Speybroeck acknowledges funding from the European Research Council under the European Community's Seventh Framework Programme (FP7(2007-2013) ERC grant agreement number 240483) and from the European Union Horizon 2020 research and innovation programme (consolidation ERC grant, agreement No 647755-DYNPOR (2015-2020)). VVS and LV acknowledge computational resources and services provided by VSC (Flemish Supercomputer Center), funded by the Hercules foundation and the Flemish Government – department EWI.

References

1 Themed issues: metal-organic frameworks, a) *Chem. Rev.* 2012, **112**, 673; b) *Chem. Soc. Rev*. 2014, **43**, 5415.
2 I. Beurroies, M. Boulhout, P. L. Llewellyn, B. Kuchta, G. Férey, C. Serre, R. Denoyel, *Angew. Chem., Int. Ed.*, 2010, **49**, 7526.
3 P. Serra-Crespo, E. Stavitski, F. Kapteijn and J. Gascon, *RSC Adv.*,2012, **2**, 5051.
4 P.G. Yot, Q. Ma, J. Haines, Q. Yang, A. Ghoufi, T. Devic, C. Serre, V. Dmitriev, G. Férey, C. Zhong, G. Maurin, *Chem. Sci.*, 2012, **3**, 1100.
5 T. D. Bennett, P. J. Saines, D. A. Keen, J. C. Tan and A. K. Cheetham, *Chem. – Eur. J.*, 2013, **19**, 7049.
6 J. Gascon, A. Corma, F. Kapteijn and F. Llabrés i Xamena, *ACS Catal.*, 2014, **4**, 361.
7 P. G. Yot, Z. Boudene, J. Macia, D. Granier, L. Vanduyfhuys, T. Verstraelen, V. Van Speybroeck, T. Devic C. Serre, G. Férey, N. Stock, G. Maurin, *Chem. Comm.*, 2014, **50**, 9462.
8 J. Rodriguez, I. Beurroies, T. Loiseau, R. Denoyel, P. L. Llewellyn, *Angew. Chem. Int. Ed.*, 2015, **54**, 4626.
9 Y. Grosu, G. Renaudin, V. Eroshenko, J.-M. Nedelec, J.-P. E. Grolier, *Nanoscale*, 2015, **7**, 8803.
10 G. Ortiz, H. Nouali, C. Marichal, G. Chaplais, J. Patarin, *Phys. Chem. Chem. Phys.*, 2013, **15**, 4888.
11 V. Eroshenko, R. C. Regis, M. Soulard and J. Patarin, *J. Am. Chem. Soc.*, 2001, **123**, 8129.
12 M. A. Saada, S. Rigolet, J.-L. Paillaud, N. Bats, M. Soulard, J.Patarin, *J. Phys. Chem. C*, 2010, **114**, 11650.
13 I. Khay, L. Tzanis, T. J. Daou, H. Nouali, A. Ryzhikov, J. Patarin, *Phys. Chem. Chem. Phys*., 2013, **15**, 20320.
14 U. Mueller, G. Luinstra, O. M. Yaghi, US Pat. 6 617 467, 2004, BASF Aktiengesellschaft.
15 E. Leung, U. Mueller, G. Cox, H. Mattenheimer, S. Blei, EP Patentanmeldung 10183283.0, 2010.
16 M. Gaab, N. Trukhan, S. Maurer, R. Gummaraju, U. Mueller, *Microporous Mesoporous Mater.*, 2012, **157**, 131.
17 F. Jeremias, D. Frçhlich, C. Janiak, S. K. Henninger, *RSC Adv.*, 2014, **4**, 24073.
18 E. Alvarez, N. Guillou, C. Martineau, B. Bueken, B. Van de Voorde, C. Le Guillouzer, P. Fabry, F. Nouar, F. Taulelle, D. de Vos, J.-S. Chang, K. Ho Cho, N. Ramsahye, T. Devic, M. Daturi, G. Maurin, C. Serre, *Angew. Chem. Int. Ed.*, 2015, **54**, 3664-3668.
19 T. Loiseau, C. Serre, C. Huguenard, G. Fink, F. Taulelle, M. Henry, T. Bataille and G. Fe´rey, *Chem. – Eur. J.*, 2004, **10**, 1373.
20 H. K. Mao, J. Xu, P. M. Bell, J. Geophys. Res., 1986, 91, 4673.
21 L. Vanduyfhuys, S. Vandenbrande, T. Verstraelen, R. Schmid, M. Waroquier, V. Van Speybroeck. *J. Comput. Chem.*, 2015, **36**, 1015.
22 Q. Ma, Q. Yang, A. Ghoufi, M. Lei, G. Férey, C. Zhong, G. Maurin, *J. Mater. Chem. A*, 2014, **2**, 99691.
23 A. Ghoufi, A. Subercaze, Q. Ma, P. G. Yot, Y. Ke, I. Puente Orench, T. Devic, V. Guillerm, C. Zhong, C. Serre, G. Férey and G. Maurin, *J. Phys. Chem. C*, 2012, **116**, 13289.
24 C. Serre, S. Bourrelly, A. Vimont, N. A. Ramsahye, G. Maurin, P. L. Llewellyn, M. Daturi, Y. Filinchuk, O. Leynaud, P. Barnes, G. Férey, *Adv. Mater.*, 2007, **19**, 2246.
25 L. Tzanis, H. Nouali, T. J. Daou, M. Soulard, J. Patarin, *Mater. Lett.*, 2014, **115**, 229.
26 N. Gokulakrishnan, J. Parmentier, M. Trzpit, L. Vonna, J.L. Paillaud, M. Soulard, *J. Nanosci. Nanotechno.*, 2013, **13**, 2847.